

Infrared Photometry for Automated Telescopes: Passband Selection

Eugene F. Milone^a and Andrew T. Young^b

^aDepartment of Physics & Astronomy, Univ. of Calgary, 2500 University Dr., N.W., Calgary, Alberta T2N 1N4, Canada;

^bAstronomy Department, San Diego State University, San Diego, CA 92115-1221, USA

ABSTRACT

We review the properties of the IRWG system of infrared stellar photometry designed to produce both high accuracy and high precision, even at moderately elevated sites. We show that it is the only broadband infrared system appropriate for sites at all elevations, and argue that this system should be used at automated as well as conventional observatories that practice precise photometry.

Keywords: Infrared, astronomical photometry, photometric system, water vapor, extinction

1. INTRODUCTION

1.1 The Promise of IR Photometry

For time-domain astronomy, for general or targeted surveys, and for a number of other explorations in ground-based astronomy, photometric precision and accuracy are required. In recent years, the infrared sky has attracted more and more attention as studies of young stellar objects, primordial planetary disks, brown dwarfs, and other cool and red objects burgeon.

Infrared photometry can yield high photometric precision because there is little Rayleigh scattering ($\propto \lambda^{-4}$), which is the main cause of atmospheric extinction in visible light. Furthermore, extinction due to aerosols, whose fluctuations are a major cause of unreliable photometry in the visible, is much smaller in the IR, as it is nearly inversely proportional to the wavelength. Although thermal emission makes the night sky bright in the IR, instruments can compensate for this (relatively high) sky brightness.

However, high IR precision has not been achieved generally, partly because photometric astronomers are reluctant to get into the IR. There are technical challenges (including low-temperature cryogenics); but the main impediment to precise ground-based IR photometry is that the filters in common use are not optimized to avoid water-vapor absorptions.

1.2 Atmospheric Windows and Evolving Passbands

Unlike visible light, infrared flux from astronomical sources can reach us only in certain spectral regions, illustrated in Fig. 1. Ground-based infrared photometry is constrained by deep molecular absorption bands (mainly due to water vapor). Infrared passbands must avoid these opaque regions, because they contribute sky emission but little transmitted flux from astronomical sources. Unfortunately, almost all previous passbands in these spectral regions (see Fig. 2) were developed *ad hoc*, without being optimized to maximize signal/noise ratio or transformability. This has degraded IR photometry and made IR transformations imprecise. It shows up directly through larger extinction coefficients and photometric variability (see Fig. 3).

The problem has been recognized ever since Johnson¹ extended the *UBVRI* photometric system to include passbands beyond $1\mu\text{m}$. He used the problematic PbS detectors that suffered from extremely low sensitivity and high dark noise. Consequently, he adopted filters with very broad spectral passbands. Indeed, the spectral

Further author information: (Send correspondence to E.F.M.)

E.F.M.: E-mail: milone@ucalgary.edu, Telephone: 403 220 5412

A.T.Y.: E-mail: aty@mintaka.sdsu.edu

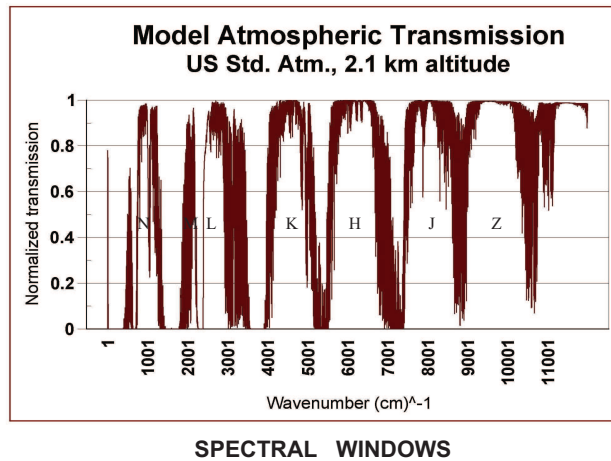


Figure 1. The transmission of light through the “windows” of the Earth’s atmosphere in the near- and intermediate infrared spectrum, computed with MODTRAN 3.7 for the U.S. Standard Atmosphere model and a site 2.1 km above sea level. Transmission is plotted against the wavenumber in cm^{-1} ($10,000/\lambda$, where λ is in μm). We have labeled the windows after the Johnson passbands that approximately filled each of them.

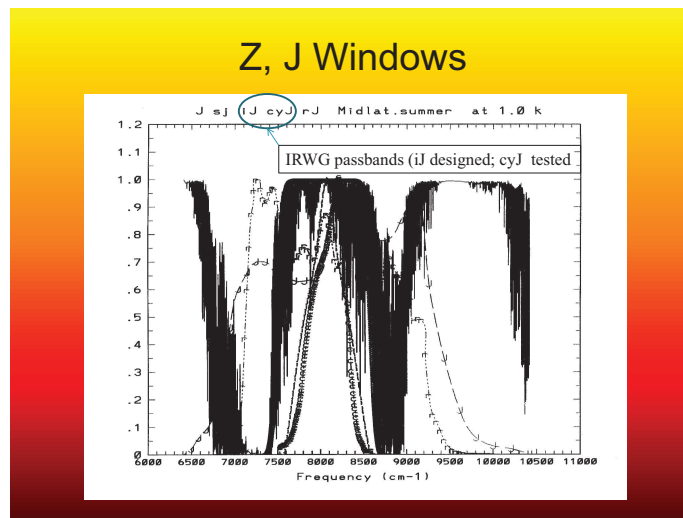


Figure 2. The Z and J windows of the atmosphere at the MODTRAN summer mid-latitude site at 1.0 km above sea level. J = the profile of the original Johnson passband; iJ , the optimized IRWG passband for this spectral region; cyJ , the filter made by Custom Scientific; rJ , a newer version of the Johnson J passband. Note how the older passbands are defined by the edges of the windows.

profiles of his J , K , and L filters overlapped opaque regions of the Earth’s atmosphere. This situation was so poor that observatories changed the specifications of the filters, to better fit them within these windows, whenever new filters were ordered. Johnson did not include, initially, a filter for the relatively clean H atmospheric window; this was added in 1968.² Nevertheless, narrowing improvements were also made to this H passband.

Cognizant that IR astronomy was failing to fulfill its promise, we began working over two decades ago to fix the problem. The time line is as follows (with a hoped-for extension into the future):

1987: Milone suggested to F. Rufener, Pres. of Comm. 25, a meeting to discuss IR extinction & standardization.

- 1988:** IAU Joint Commission meeting at Baltimore General Assembly identified the main problem and recommended action; a Working Group spearheaded by Young was formed.
- 1991:** McLean commissioned a formal Infrared Working Group (*IRWG*).
- 1992:** Preliminary results reported³ at IAU Colloquium 136.
- 1993:** Barr Associates offered but did not deliver prototype filters.
- 1994:** YMS paper⁴ in A&AS presented the recommended optimized passbands.
- 1999:** IRWG filters made by Custom Scientific Corp.
- 2002:** Simons' Gemini filters⁵ designed (MKO-NIR); but a mass buy of these unoptimized filters was organized⁶ for all IR observatories.
- 2005:** The IRWG system was realized^{7,8} through observational trials and a preliminary list of standards.
- 2008;** IRWG passbands promoted to both professional and amateur observatories.⁹
- 2012:** Mass buy of Near-IR IRWG filters?
- 2012:** Longer-wavelength IRWG filters produced, used?

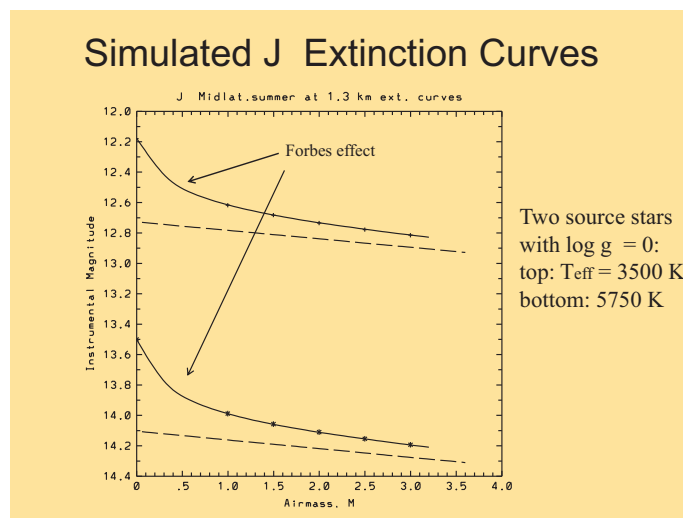


Figure 3. A simulated extinction curve computed for a summer, mid-latitude atmospheric model for a site 1.3 km above sea level. This passband is the original Johnson *J*. The two flux sources are stellar atmosphere models¹⁰ with effective temperatures of 3500 K and 5750 K. The dashed lines are the curves' asymptotes at very high airmass. Note the strong curvature between 0 and 1 airmass; this curvature is both unknown and unknowable when ground-based observations are made. Moreover, the water vapor column varies with time, so the actual extinction curve can vary greatly in the low-airmass corner. The production of such plots was discussed in earlier papers;⁴ see especially an earlier paper advocating the IRWG passbands for IR photometry with robotic telescopes.¹¹

1.3 The Advantages of the IRWG Passbands

As a result of this effort, we now have IR passbands that yield relatively straight extinction lines (as in Fig. 4) and have spectral profiles with much smaller slopes than those produced by the old Johnson passbands and nearly all of their unoptimized successors. The slope is important to assure good transformations among data obtained with filters from different batches, allowing for manufacturing tolerances.

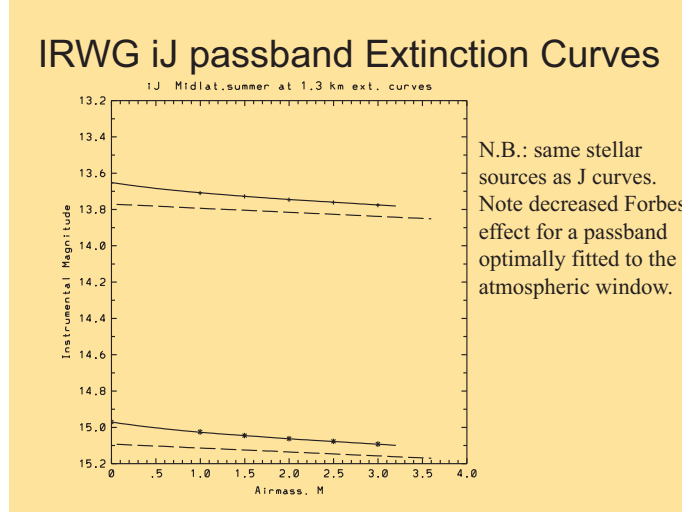


Figure 4. Contrast these extinction curves with those of Figure 3 of the J passband. The reduced Forbes effect with the iJ passband means that variations in water vapor, which have played havoc with photometry carried out with the severely impaired J passband, will have minimal effect on this passband. Similar differences will be expected between this and all unoptimized passbands.

The IRWG passbands are not defined by the edges of the atmospheric windows, so they admit no flux from these (constantly varying) edges. Eliminating the varying edge regions eliminates the main sources of variation (i.e., noise) in observational data, and allows the promise of high precision to be realized. There are two costs of this improved precision: first, lower throughput; and second, higher prices for the filters, if made in small lots.

But these costs are a good trade-off, because we are buying:

1. higher precision;
2. improved signal-to-noise ratio;
3. lower extinction;
4. minimal curvature of the extinction curve high in the atmosphere, which yields higher precision and accuracy in extra-atmospheric magnitudes.

2. A CLOSER LOOK AT EXTINCTION

The parts of any IR bandpass that are blocked by the strongest telluric absorption have the highest monochromatic extinction in that passband, so flux is removed from these spectral regions high in the atmosphere; the remaining flux is in regions of lower average absorption. Thus, the total passband extinction increases less and less rapidly with increasing airmass (actually, water-vapor-mass). This decrease in incremental extinction with increasing airmass is the Forbes¹² effect, and is obvious in synthetic extinction curves (e.g., Fig. 3), which are curved rather than straight. The largest change in curvature occurs in the unmeasurable interval between 0 and 1 airmass. In these plots, passbands prefixed with “y” or “i” are those of the IRWG set; those with “c” are the profiles of the IRWG filters produced by Custom Scientific Corp. of Phoenix, AZ. Results for other filters in common use over the past three decades are also shown. The curves in the figures represent an interpolation formula proposed by Young,¹³ and later put into a more convenient form.^{3,4}

Extinction changes the spectral flux distribution from an astronomical source with increasing airmass. If we consider that distribution as a Hilbert-space vector, whose direction changes as the transmitted flux decreases, its rotation angle, θ , measures the atmospheric modification of the passband. Fig. 5 illustrates the relationship between θ and another measure of the Forbes effect, the difference in transmission between 0 and 1 airmass.

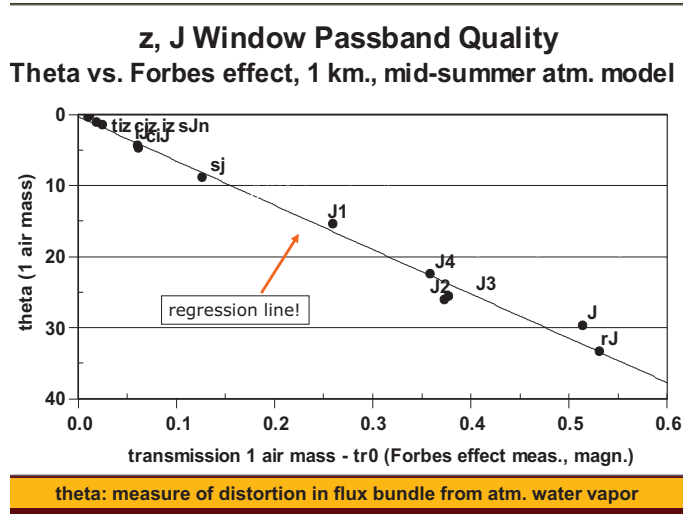


Figure 5. Here we plot θ , a figure of (de)merit, which increases with filter impairment, against the difference in extinction between 0 and 1 air mass; both are measures of the Forbes effect. The Z-window passbands are in the upper part of the diagram: *iz* is the recommended IRWG passband; *tiz* is a trapezoidal passband otherwise similar to *iz*; *ciz* is the Custom Scientific Corporation replication of the *iz* passband. *sJn* is the Selby narrow-band filter¹⁴ placed in a very narrow region of the *J* window and used for calibration purposes only; *sj* is Simons' Mauna Kea *J* passband, designed for use with the Gemini telescopes; *J1*–*J4* are modifications to the original Johnson passband, *J*, used at various observatories in the 1990s; *rJ* is an early version of the *J* filter, formerly used at the Rothney Astrophysical Observatory.

2.1 Relationship between SNR and Extinction

Atmospheric absorption affects the uncertainty (noise) in IR photometry in two ways. First, the absorption decreases the detectable stellar flux; but it does so in a varying way, because water vapor (the main absorber) varies from night to night, and even from minute to minute. These variations in absorption produce variations in the detectable signal throughout the infrared.

Second, the sky brightness varies, because thermal emission from water vapor is a major contributor to the sky radiance at wavelengths longer than about $3 \mu\text{m}$. Although some of this variable background can be removed by chopping and other compensating techniques, the removal is never perfect. As a result, when detector noise is made negligible by cooling, water-vapor fluctuations in both absorption and emission are usually the major source of random error in IR photometry.

We have published⁷ the thermal atmospheric emission as well as the transmission through all of the IR passband profiles that we were able to obtain, along with a measure of the signal-to-noise ratio (SNR), and synthetic extinction curves. This presentation was augmented in 2007⁸ and 2008.⁹ With these data we demonstrated the strong connection between increased SNR and decreased extinction. These are illustrated for the Z- and J-window passbands in Fig. 6.

3. IR PHOTOMETRY AT ALL PHOTOMETRIC SITES

In general, scientific data should be independently reproducible. In particular, an open photometric system¹⁵ should be reproducible at most astronomical observatories; a system in which data can be obtained only at a single site is of limited utility, especially for variable-star work, where longitude coverage is often essential.

When Simons and Tokunaga⁵ presented the results of an IR filter design study for the Gemini telescopes, they attempted to compromise between the specifications set forth by the IRWG⁴ and a desire to maximize throughput, weighting their selection highly by the latter. The result is again a series of passbands that butt up against the edges of the windows, even at a site with 1-mm of precipitable water vapor and the 4.2 km elevation

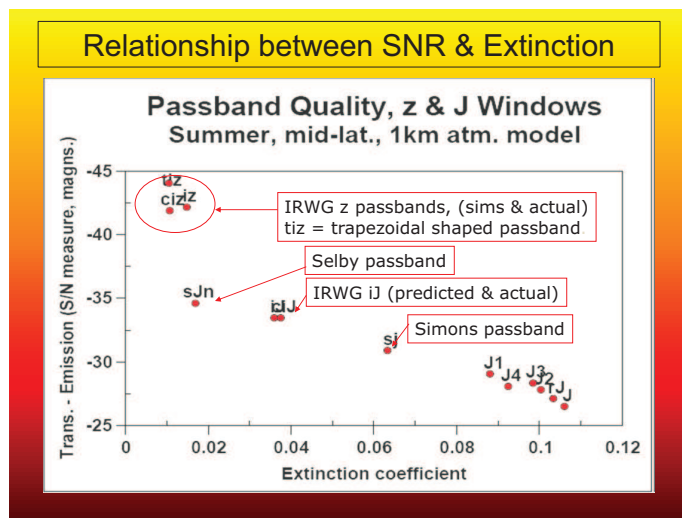


Figure 6. A measure of the signal-to-noise ratio (the difference between the transmission and emission at one airmass, in units of magnitude), plotted against the extinction coefficient between 1 and 3 air mass. Note that the older passbands have the lowest SNR and highest extinction; the new Z-window bands have the highest SNR and lowest extinction; and the *iJ* (target) and *ciJ* (produced) IRWG bands have the highest SNR and lowest extinction of all the J-window passbands tested. Selby’s very narrow calibration J passband¹⁴ falls in a unique region of the plot, and Simons’ Gemini J passband lies between the optimized *iJ* and the old passbands.

of Mauna Kea. As we have noted,⁷ this is not a good idea, especially when these filters are then recommended to observatories at lower elevations and with higher amounts of water vapor.

Moreover, the specified⁶ properties and tolerances of these filters show that two of them compromise the passbands even more. The first is the relaxation of the leak restriction from 10^{-5} to 10^{-4} , done solely to keep the cost down. Second, they specify a sharp roll-off of $< 2.5\%$, instead of more gradual slopes that would both diminish the effect of water-vapor absorption at the edges of the passband, and increase the likelihood of good transformations between filters from different batches, where shifts in central wavelength and width can be expected.

Thus, in their efforts to improve IR photometry, they fell into the same trap as previous generations of IR passband-modifiers. In doing so, they *did* improve IR photometry for the highest and driest sites — though not optimally; but in queering the pitch, so to speak, they blocked general adoption of truly optimized passbands with superior SNR and other properties.

Near-IR IRWG photometry is now possible at both high- and low-elevation sites (if good visible-spectrum photometry is already done there) — but photometry done at high, dry sites can also benefit from improved accuracy and transformability. Fig. 7 shows how well the near-IR bands fit within the atmospheric windows, even at a low-elevation site. Formerly, it has been very difficult to do precise IR work at any site, and few contemplated doing so at lower elevation sites. With optimized passbands, this is no longer the case; such data should be transformable to observations made at higher and drier sites.

If the IRWG filters are made widely available, they will be used!

4. DETAILS OF THE IRWG SYSTEM

Although the specifications for the IRWG passbands have been given in several publications already, we reproduce them here in Table 1 for convenience.

The filters should be blocked to both short- and long wavelengths, with leakage at 10^{-5} at worst. The roll-off should be gradual, placing the smallest sensitivity at the edges of the passband, so that the variations in absorption produced by changes in water-vapor content have minimal effect on the throughput. Hence, the

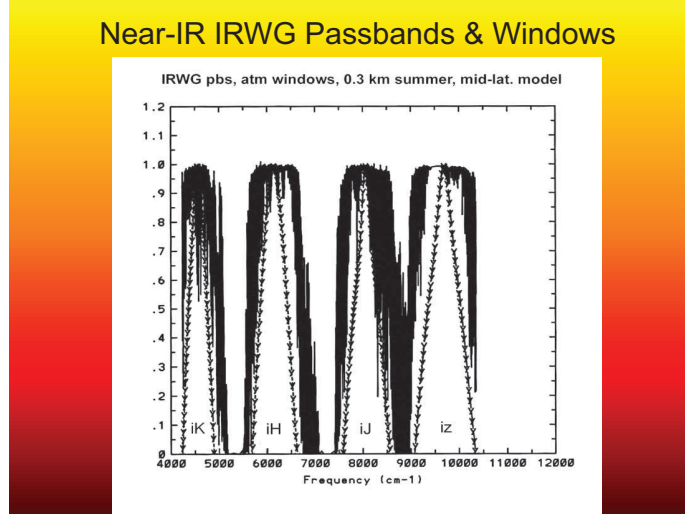


Figure 7. The near-infrared suite of IRWG passbands superimposed on the transmission spectrum of a mid-latitude summer atmosphere model for a site at 0.3-km elevation.

Table 1. Wavelength Specifications (in μm) for the IRWG Filters Profiles

Passband	iz	iJ	iH	iK	iL	iL'	M	in	iN	iQ
5%	0.970	1.170	1.514	2.047	3.374	3.654	4.564	8.731	9.756	16.656
50%	0.996	1.202	1.555	2.100	3.483	3.763	4.618	8.873	10.100	17.106
80%	1.016	1.225	1.585	2.141	3.554	3.834	4.652	8.968	10.369	17.439
100%	1.032	1.240	1.628	2.196	3.620	3.900	4.675	9.030	11.100	17.900
80%	1.047	1.254	1.672	2.240	3.686	3.966	4.698	9.101	11.832	18.329
50%	1.069	1.280	1.707	2.288	3.757	4.037	4.732	9.196	12.100	18.712
5%	1.099	1.315	1.754	2.353	3.882	4.162	4.784	9.339	12.444	19.231
FWHM(\AA)	730	790	1520	1888	2740	2740	1140	3230	20000	16060
FWHM/ λ_{peak} (%)	7.1	6.4	9.3	8.6	7.6	7.0	2.4	3.6	18.0	9.0

preferred shape of the passbands is triangular, as seen in Table 1, and in Fig. 7. We note that in some passbands, a slightly trapezoidal shape may be slightly beneficial; but, in most cases, our numerical experiments indicate this not to be so.

4.1 Overcoming Impediments

Impediments to IRWG use are not severe: SNR varies inversely with both extinction and with a measure of the Forbes effect. Therefore, a small loss of raw throughput is recouped in signal-to-noise gain. Reduced costs can be realized through bulk orders with uniform filter specifications. We encourage wide use at IR observatories, to build a large body of observed data and enlarge the list of standards.

We think that infrared astronomy has progressed from the days of “white-light” photometry where essentially no filter was used (this is effectively the case where the edges of the atmospheric windows define the spectral bandwidth), and that most modern astronomers are more concerned about the signal-to-noise ratio rather than the raw throughput. This is certainly the case in visible-light photometry where unfiltered photometry is done only in some single-camera surveys. Slowly it is being recognized that this is the situation in the eight atmospheric windows of the near and intermediate infrared.

Automated IR systems with these passbands could establish a post-Johnson system more widely, creating a larger body of data to which future observations will be more accurately transformable. More purchases will make the filters cheaper to purchase.

4.2 Near-IR IRWG Passbands and Windows

Figs. 4–6 have already shown results for the Z and J windows; but see also Figs. 8 and 9. The former demonstrates the superb quality of the *iz* passband, and the latter compares the theta values at 1 and 3 airmasses of several passbands for three atmospheric models.

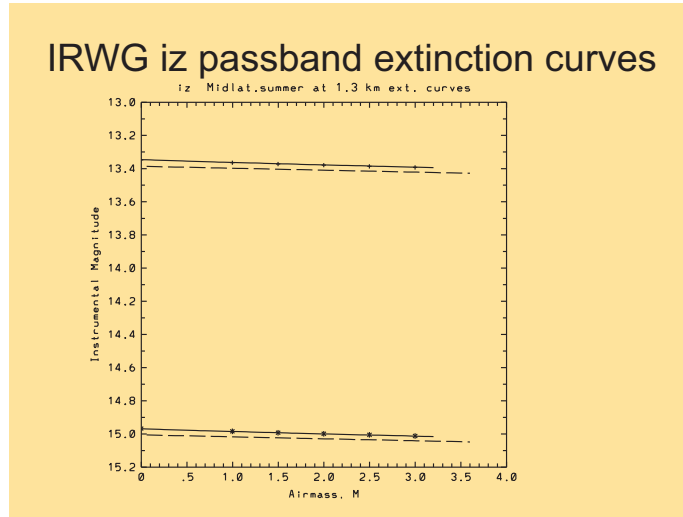


Figure 8. The simulated extinction curve for the *iZ* passband computed with mid-latitude summer atmosphere model for an elevation of 1.3 km. Note that there is little difference between the large-airmass asymptote and the extinction curve itself; so data taken in this passband may be reduced to outside atmosphere with a straight Bouguer line.

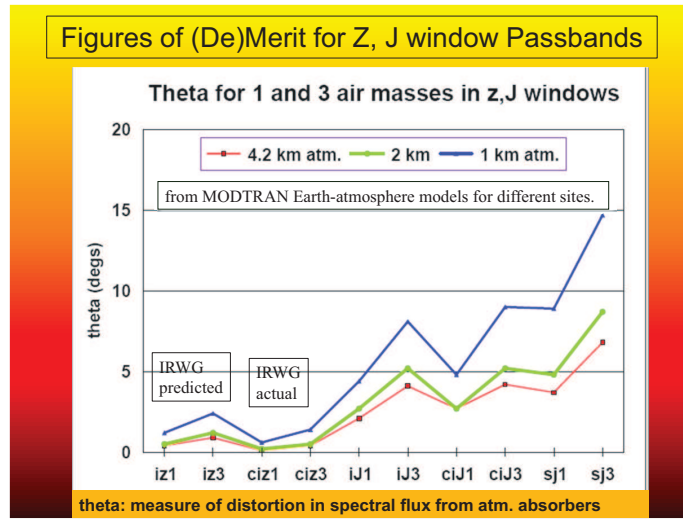


Figure 9. The quantity θ for the *iz*, *ciz*, *iJ*, *ciJ*, and the Simons *J* passband designed for use with the Gemini telescopes, for both 1 and 3 air masses. The results are shown for three atmospheric models: a tropical model at 4.2 km elevation, the standard-atmosphere model at 2 km elevation, and a mid-latitude summer model at 1 km elevation.

For the simulations and properties of the H-window passbands, see Figs. 10–12.

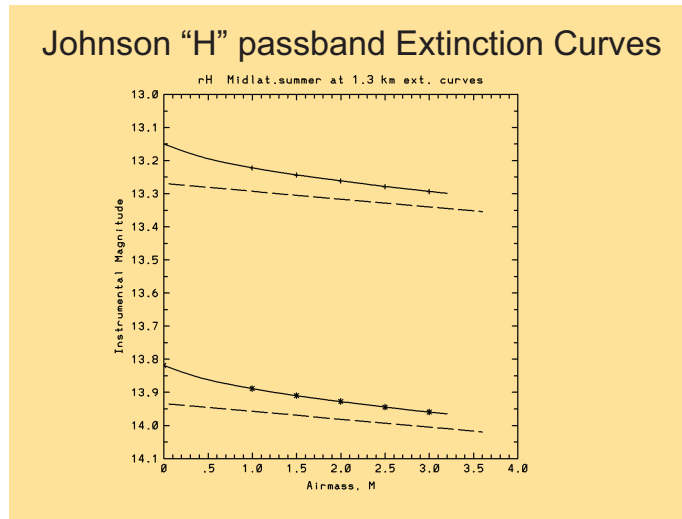


Figure 10. Simulated extinction curves for the Johnson H passband computed with a mid-latitude summer atmospheric model for a 1.3-km elevation site. The Forbes effect is smaller than for J and the longer-wavelength Johnson passbands, because the H window is relatively clean.

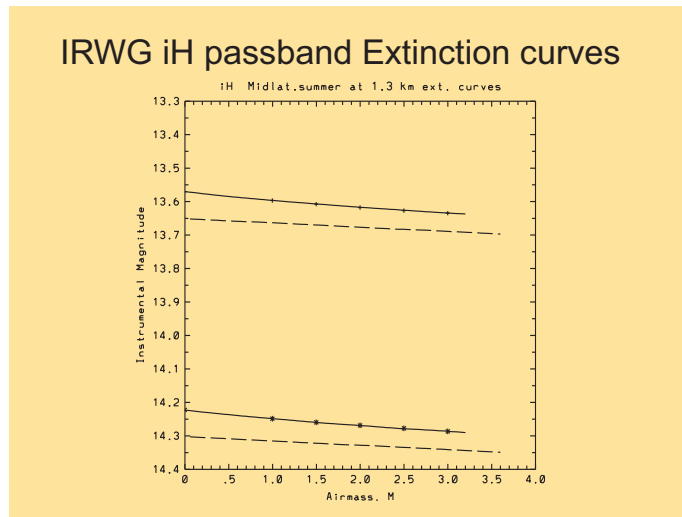


Figure 11. Simulated extinction curves for the IRWG iH passband. The atmospheric model and site are the same as for the previous plot. Note that the Forbes effect is still less.

The K window is less clean than the H window, and has a water-vapor feature mid-window, near 4600 cm^{-1} ($2.17\ \mu\text{m}$). The blue edge of the window is defined by carbon-dioxide bands ~ 4850 and 4970 cm^{-1} (2.06 and $2.01\ \mu\text{m}$, respectively). Even some of the more recent passbands (cf. Figs. 15–17), such as those of Skrutskie¹⁶ and Simons and Tokunaga,⁵ intrude on these bands, which do not decrease rapidly with increasing elevation, unlike water-vapor bands.

Optimized passbands should be triangular, to minimize both the effects of absorptions at the edges of the window, and transformation errors between filters from different production runs. Figs. 13 and 14 show how we optimized⁴ the K-window passband, iteratively adjusting its position and width to maximize SNR.

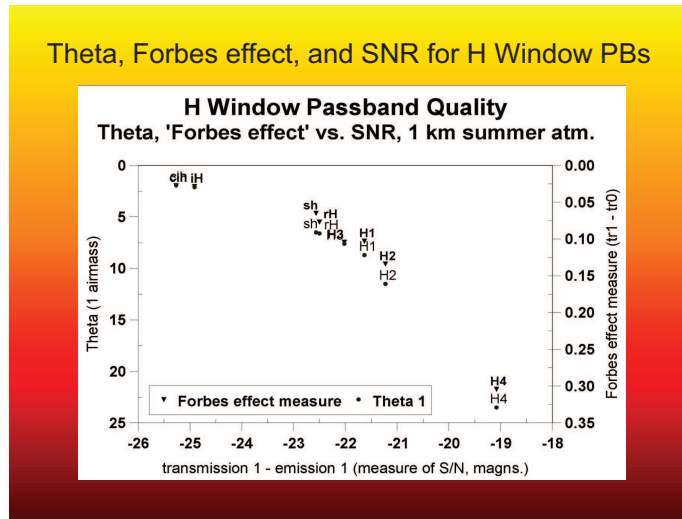


Figure 12. Note the improvement of the (de)merit parameter θ and signal-to-noise ratio for the IRWG iH and Custom Scientific Corporation's realization of it, ciH , over previous passbands. The Simons H passband, sh , designed for the Gemini telescopes, falls near the better H passbands of the past.

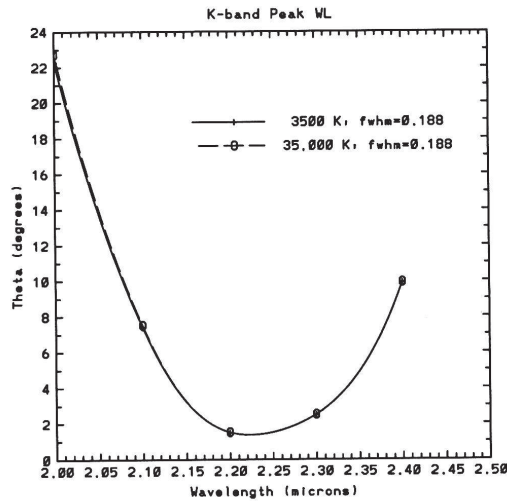


Figure 13. The example of WL-placement optimization simulation shown here is for a tropical atmosphere model for a site at 4.2 km elevation. For these tests, two stellar sources (Kurucz models) were used. The quantity θ , a measure of the Forbes effect, is to be minimized, so a series of profiles with different central wavelengths were run. The minimum of the curve is close to 2.20 microns, for a FWHM of 0.100 μm . Thermal emission increases to the red, however, so that a slightly greater SNR is achieved by shifting the maximum slightly to the blue.

4.3 Measured Extinction in the IRWG near-IR Passbands

How do the simulations compare to real data? Extinction was measured through versions of the old Johnson JHK filters and through the IRWG passbands (iz , iJ , iH , and iK), on the same night at the Rothney Astrophysical Observatory, located at 51° N and at an elevation of 1.3 km.

The extinction coefficients were 0.02, 0.05, 0.02, and 0.05 mag./airmass for iz , iJ , iH , and iK , respectively (see Fig. 18). Those for the Johnson passbands (Fig. 19) were much larger: 0.08, 0.05, 0.11 mag./airmass for

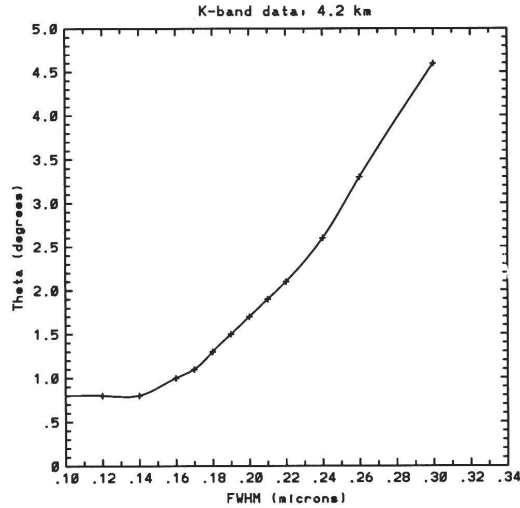


Figure 14. FWHM optimization for a tropical atmosphere model at 4.2 km elevation. θ increases with width, as expected. The optimum width is set below the inflection point of the curves by a standard deviation, to allow for variation in filter manufacture.

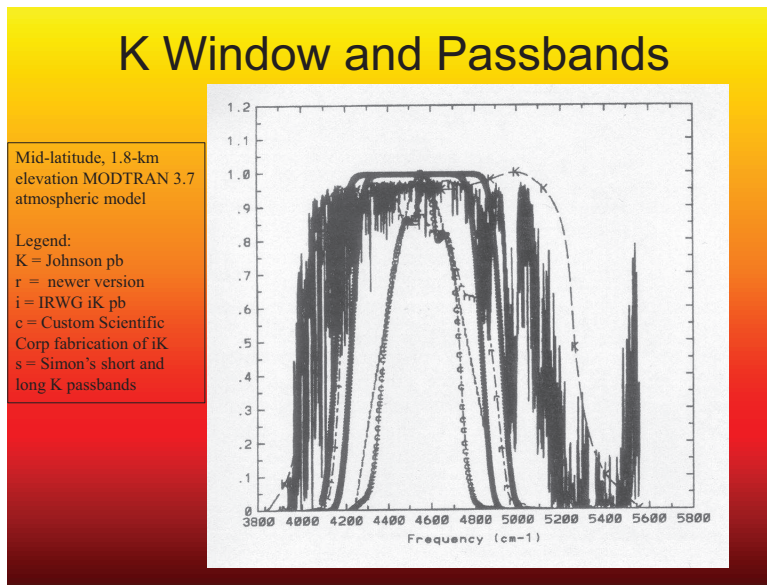


Figure 15. The atmospheric K window computed for a mid-latitude standard model atmosphere at 1.8 km elevation. A number of passbands are shown: K = Johnson; $r = rK$, a more recent version of K ; $i = iK$, the IRWG recommended passband for this window; $c = ciK$, the Custom Scientific Corporation replication of iK ; $s = sk$ and sl , the Simons short- and long- K passbands designed for the Gemini telescopes. Note how the latter are still defined by the Earth's atmosphere.

the Rothney J , H , and K passbands.

Even if one is unconvinced by our exhaustive numbers of simulations, these observations along with the relationships among θ , SNRs, the Forbes effect, and extinction, should convince even the most recalcitrant IR astronomer that SNR should trump pure throughput, and that precise photometry can be achieved reliably only with optimized passbands.

We can summarize the first part of this paper as follows. All Johnson IR passbands suffer from effects of

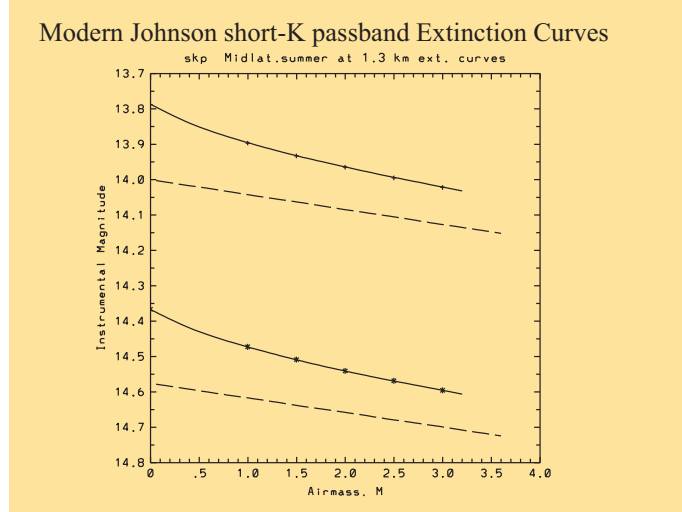


Figure 16. Simulated extinction curve for the Simons short- K passband from the near-IR Mauna Kea set, computed with the MODTRAN 3.7 atmosphere model for a mid-latitude, summer site at 1.3 km elevation.

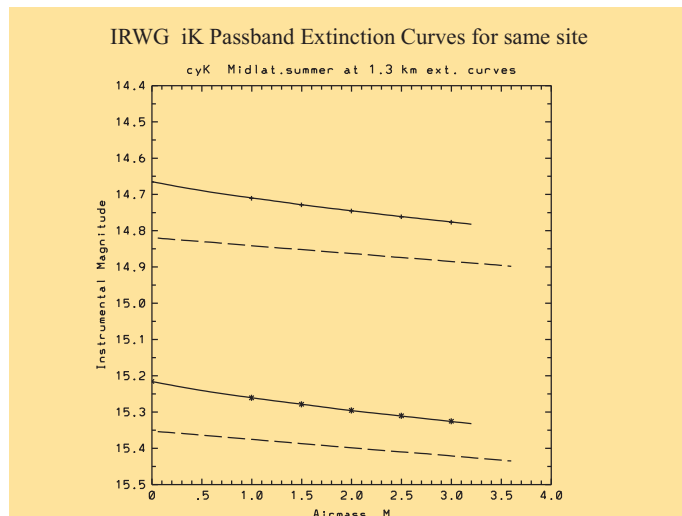


Figure 17. Extinction curves for the $cyK = ciK$ passband for the same site as Fig. 16. Note the decreased Forbes effect.

water vapor absorption: non-linear extrapolation to 0 AM is needed, because of the Forbes effect. Both the MKO-NIR and the IRWG passbands reduce exposure to water vapor effects at MKO; but at lower-elevation sites, the IRWG bands are much more effective. The IRWG^{4,7} passbands offer improved SNR, extinction, and transformation from sites at a considerable range of different elevations and for a range of terrestrial atmosphere models.

We describe the historical development of IR astronomy elsewhere;¹⁷ we think that widespread use of the IRWG passbands will be the next important development of infrared astronomy.

5. THE LONGER-WAVELENGTH PASSBANDS

Here we show that the longer-wavelength IRWG passbands should be replicated and tested for intermediate-IR photometric precision. Fig. 20 shows the behavior of the L-window passbands we have tested. We found optimal

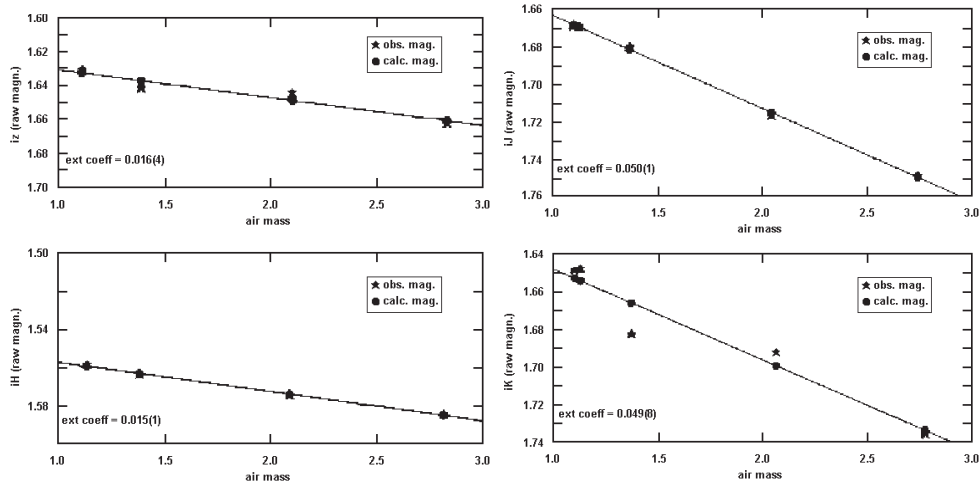


Figure 18. Extinction plots of Vega for the night of 2000 Sept. 26 in the IRWG passbands *iz*, *iJ*, *iH*, and *iK*, revealing Bouguer coefficients of 0.0164 ± 0.004 , 0.050 ± 0.001 , 0.015 ± 0.001 , and 0.049 ± 0.008 , respectively. This and Fig. 19 are reproduced here with the permission of the JAAVSO.⁹

passbands for both the red and blue parts of the L window (*iL* and *iL'*, respectively).

The severely impaired M window (see Fig. 21) presents major challenges, even at 4.2 km, as Fig. 22 shows. But even here, optimization produced an improved passband, *iM*, as the extinction curves in Fig. 23 indicate. Figs. 24 and 25 show its performance at lower elevations.

The N window, near $10 \mu\text{m}$, is relatively clean at 4.2 km (see Figs. 26 and 27), so for this window the optimum passband, *iN*, is very wide, $20,000 \text{ \AA}$. Yet the extinction curve (Fig. 28) for this passband has only a very slight Forbes effect, even in low elevations in a summer, mid-latitude atmospheric model (see Figs. 29 and 30). The narrower *in* passband (Fig. 31) at the blue side of the window is not as good.

We have nothing to add to our previous discussion⁴ about the Q window, and, although we recommend the optimized *iQ* passband for this window, no broad passband in this window can be free of the Forbes effect, even at high elevation sites and in the driest conditions. The specifications for this passband are nevertheless given in Table 1; we recommend its use exclusively for high-elevation sites under very dry conditions.

For the passbands beyond the L window, the current detector of choice is the bolometer, which is traditionally cooled with liquid helium; this requires yet more expertise in cryogenics to handle safely and effectively. There are, however, closed systems of such cryogenics which can facilitate operations.

6. THE FUTURE OF IRWG WORK

6.1 Extinction monitoring

Real-time monitoring of water-vapor extinction, as recommended at the Baltimore¹⁸ meeting, could be especially beneficial for the *iM* and *iQ* passbands, and the old, unoptimized passbands still in use. Such monitoring should involve a dedicated telescope, probably aimed at a star close to the pole.

6.2 Further Consideration of the Z Window Passband

The *iz* passband FWHM is optimized, but the θ parameter is so small, that for higher elevation sites, it might be broadened somewhat without great loss in transformability with data through the specified *iz* passband at lower elevation sites. The 730 \AA FWHM specification has the additional benefit that optical detectors have declining sensitivity on the long-wavelength side, so that not much flux is lost at that part of the passband if these detectors are used. However, recent advances in detector technology have slightly improved the passband

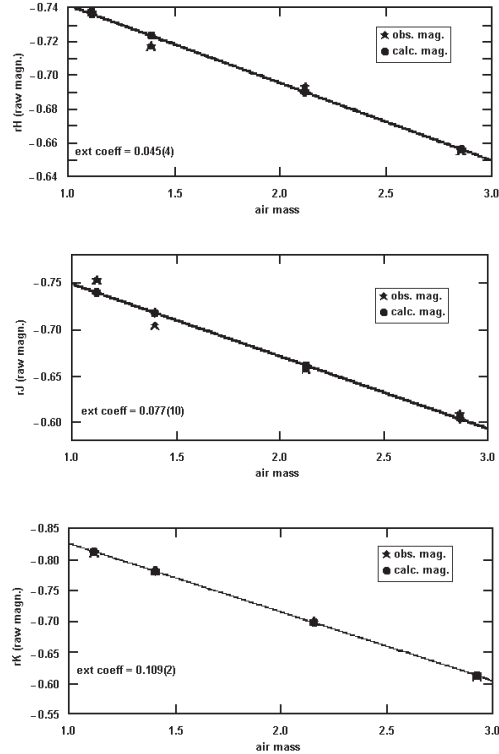


Figure 19. Extinction plots of the same star, Vega, and for the same night, 2000 Sept. 26, in an older set of passbands, rH , rJ , and rK , similar to the original Johnson passbands. The extinction coefficients are: 0.045 ± 0.004 , 0.077 ± 0.010 , and 0.109 ± 0.002 , respectively. Compare these values with those in the IRWG passbands. The data for both this and the preceding plot were obtained at the Rothney Astrophysical Observatory in the foothills of the Canadian rockies at an elevation of 1.3 km.

coverage. In addition, the photometry described in our 2005 paper⁷ was carried out with an InSb detector, which is flat across this passband. Thus a modest broadening of this passband could be contemplated.

6.3 Light curves

Some of the motivation for this extensive project has been the expected boon for variable star photometry, where the expected improvement of precision of resulting light curves could, potentially, match the extraordinary improvements in lightcurve analysis techniques and software discussed, for example, by Milone and Kallrath.¹⁹ In this paper, we have argued for improved light curve precision in order to obtain improved accuracy as well as precision in light curves and in the resulting parameter determinations.

Sub-millimagnitude precision would be especially valuable for eclipsing binary systems with cool components. Minimal color effects and temperature sensitivity will enable more precise fundamental data than has been possible heretofore. IR light-curve acquisition has been attempted at the RAO in recent years, but for a variety of reasons involving major observatory innovations, encoder reliability issues, and deteriorating interference filters, this task could be carried out only sporadically. Such work needs to be carried out with newly fabricated filters to be sure that the gains expected from our simulations and standardization work can be fully realized.

6.4 Help wanted

These suggestions depend on the work of the future IRWG. So, if you are interested in joining the struggle to improve infrared photometry, join the IR Working Group! Contact the authors to apply, and you will be welcomed!

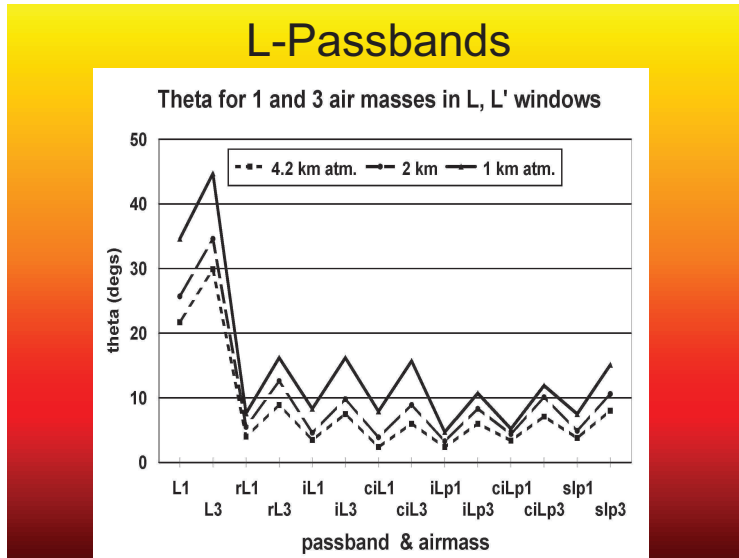


Figure 20. The values of θ computed for two air masses and three atmospheric models for bands in the L-window: Johnson passband (L), a slightly newer version (rL), the recommended IRWG passbands (iL and iLp), the Custom Scientific Corporation production of these passbands (ciL, ciLp), and the Mauna Kea L' passband (slp).

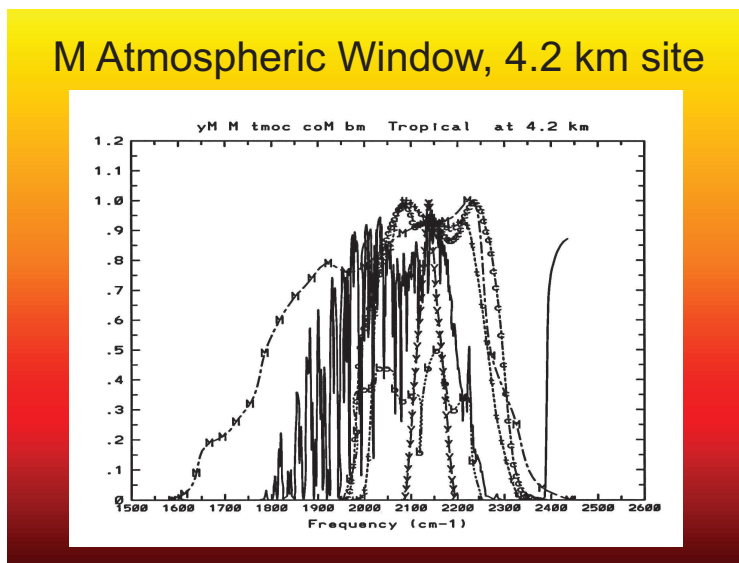


Figure 21. The M atmospheric window computed for a tropical site, 4.2 km above sea level, and the profiles of passbands: the original Johnson M , the IRWG recommended passband ($yM = iM$), and three other passbands used in the 1980s and 90s ($tmoc$, coM , and bm).

ACKNOWLEDGMENTS

This work has been supported in part by grants to EFM by the Canadian Natural Sciences and Engineering Council, the Physics & Astronomy Dept. of the University of Calgary, the University of Calgary Research Grants Committee, the students of the Advanced Astrophysics Laboratory course who helped with observing, and the Infrared photometry community, including those who provided passband profiles for study. We acknowledge also the assistance of the CFHT-AFAR LOC for support to EFM.

Johnson M passband extinction, 4.2 km site

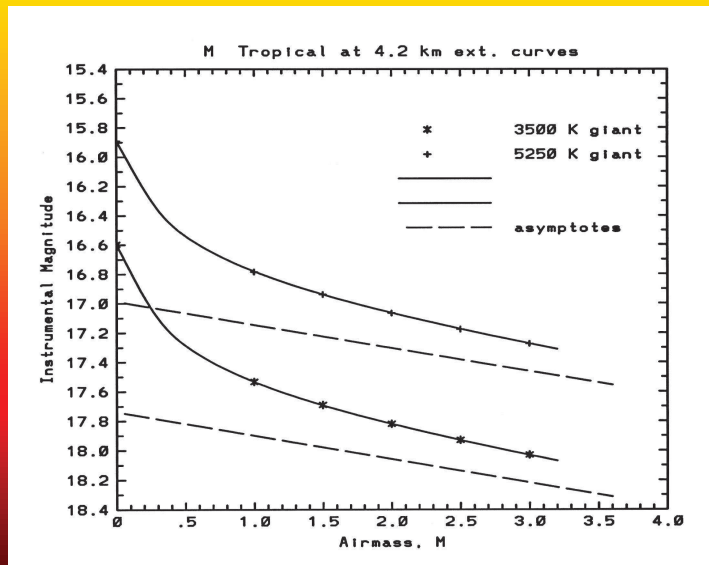


Figure 22. The extinction curves for the Johnson M passband for a tropical atmospheric model for a site 4.2 km above sea level. Note the enormity of the Forbes effect for this badly-impaired passband in a very obscured window.

IRWG iM passband extinction, 4.2 km site

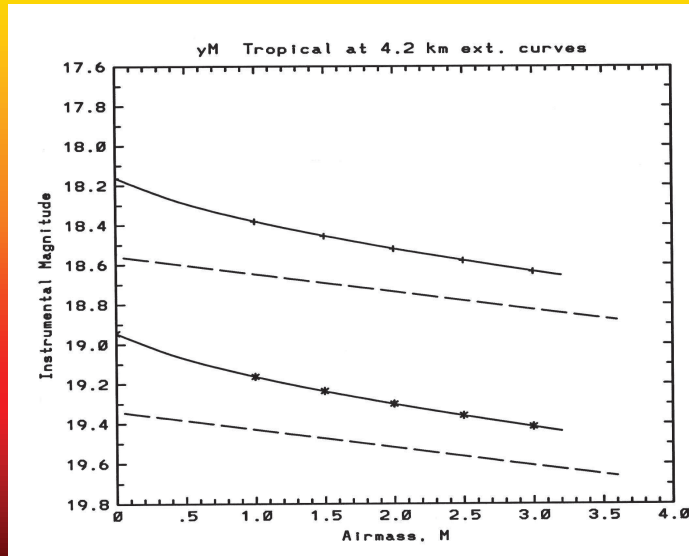


Figure 23. The extinction curves for the $yM = iM$ passband for the same site as the previous figure. Note the decrease in the size of the Forbes effect.

M Atmospheric Window, 2 Km site

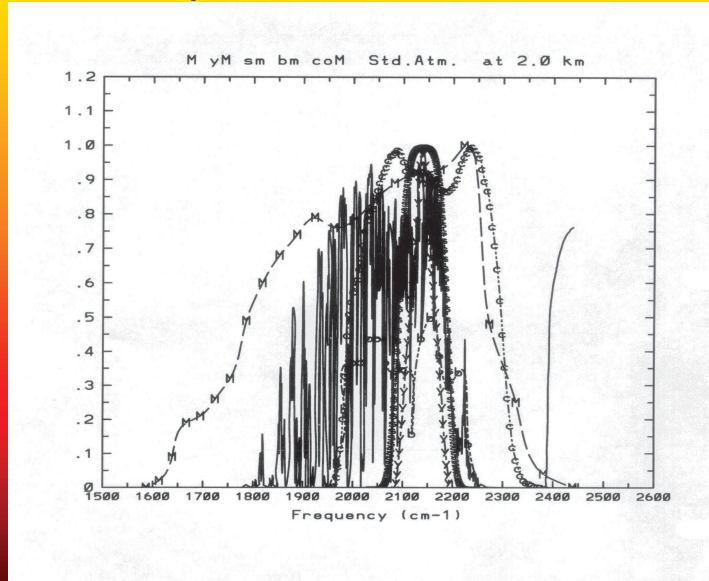


Figure 24. The M atmospheric window for the standard atmosphere at 2 km above sea level, and passband profiles: Johnson M , the IRWG passband ($yM = iM$), and three other passbands used in the 1980s and 1990s (sm , bM , and coM). Note that the window is more obscured in this model than that for the 4.2 km site.

IRWG iM passband extinction for RAO

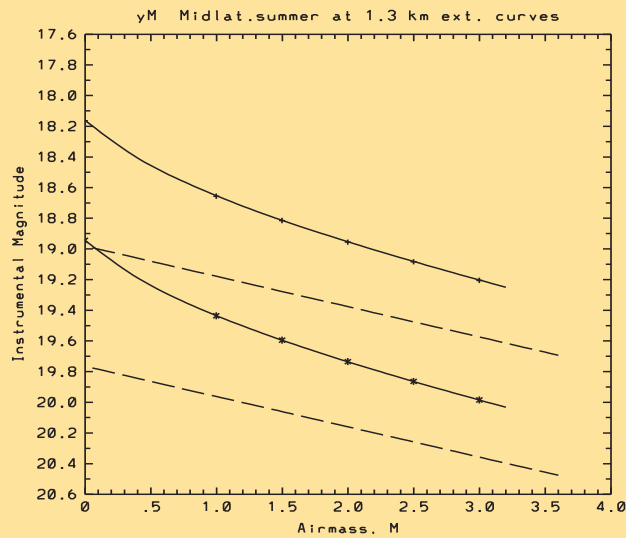


Figure 25. The extinction curves for the $yM = iM$ passband for a mid-latitude, summer atmosphere model, and for a site only 1.3 km above sea level. Note the decrease in the size of the Forbes effect compared to Fig. 22, even though the window is even more impaired than in Fig. 24.

N Atmospheric Window, 4.2km site

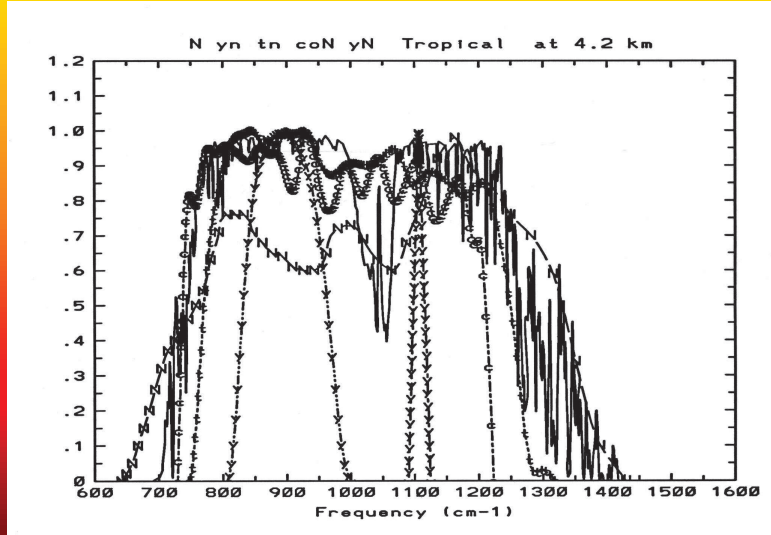


Figure 26. The N atmospheric window computed for a tropical site 4.2 km above sea level, and the profiles of passbands: the original of Johnson N , the IRWG passbands ($yN = iN$, and $yn = in$), and two other bands used in the 1980s and 1990s (tn , coN).

Johnson N Passband extinction, 4.2km site

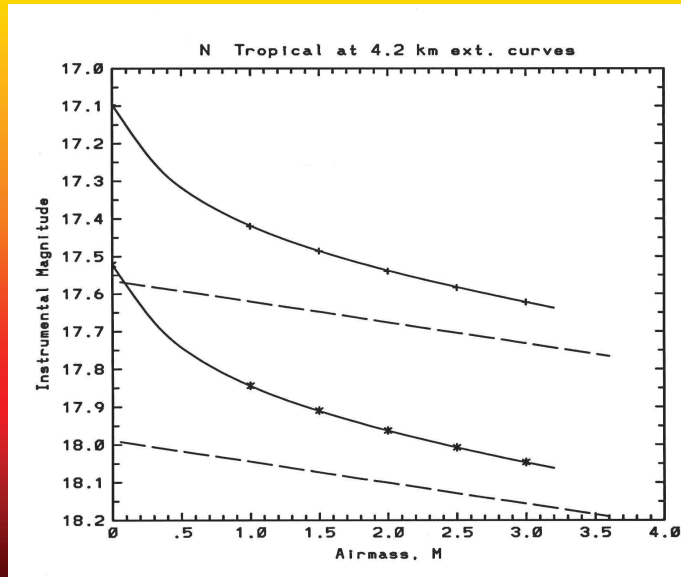


Figure 27. The extinction curves for the Johnson N passband, for the same atmospheric model and site as in the previous figure. Note the large Forbes effect.

IRWG in Extinction, 4.2km site

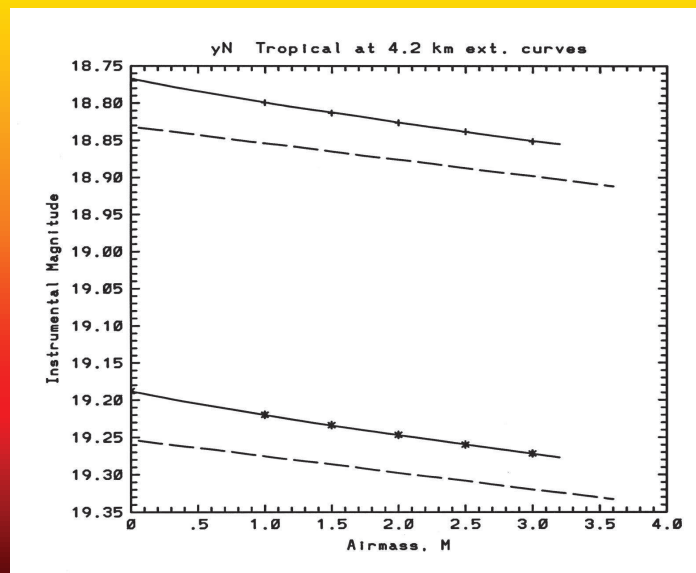


Figure 28. The extinction curves for the iN passband for the same atmospheric model as in the previous figure. Note the great decrease in the size of the Forbes effect, so that a linear extinction correction appears to be feasible.

Johnson N passband extinction, 1.3km site

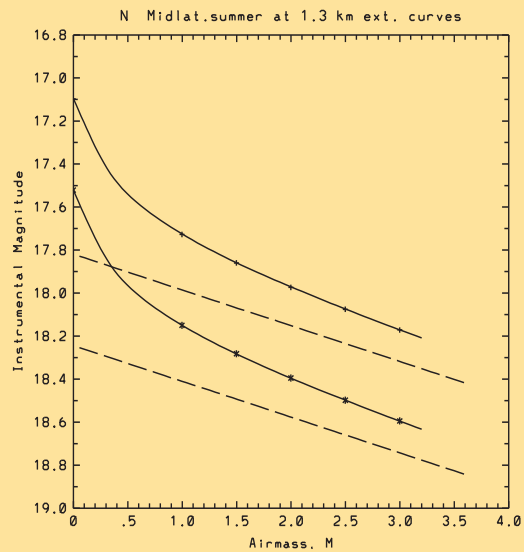


Figure 29. The extinction curves of the Johnson N passband, as in Fig. 27 but for a mid-latitude, summer atmosphere model for a site 1.3 km above sea level.

IRWG *iN* Extinction, 1km site

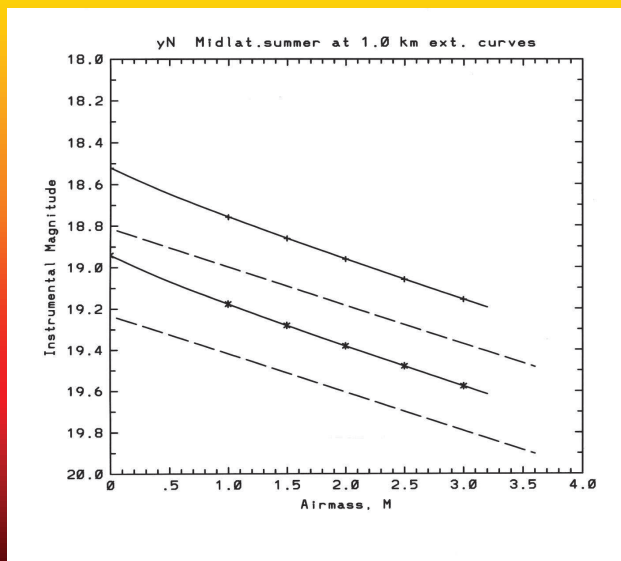


Figure 30. The extinction curves for the *iN* passband for the same atmospheric model as in the previous figure, but at an even lower elevation, 1 km. Note the decrease in the size of the Forbes effect. Such a result implies that high-precision photometry may be possible in the *iN* passband even at low-elevation sites.

IRWG *in* passband extinction for 1.3km site

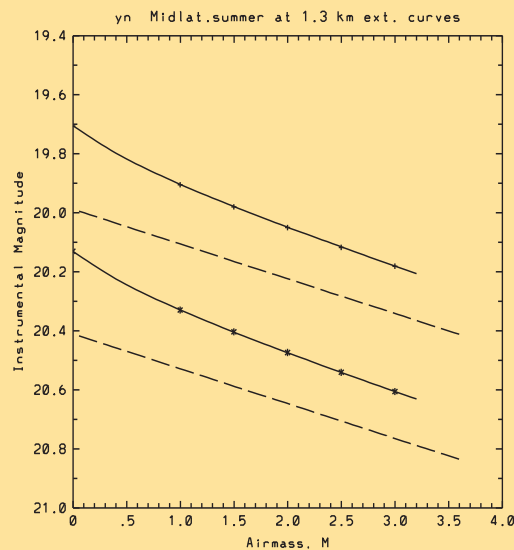


Figure 31. Extinction curves for the *in* passband of the IRWG set. Even for such a low-elevation site, this auxiliary passband could be used, but photometry would be better at higher-elevation sites.

REFERENCES

- [1] H. L. Johnson, B. Iriarte, R. I. Mitchell, and W. Z. Wisniewski, "UBVRIJKL photometry of the bright stars," *Comm. Lunar Plan. Lab.* **4**, 99–110, 1966.
- [2] H. L. Johnson, J. W. MacArthur, and R. I. Mitchell, "The spectral-energy curves of subdwarfs," *Astrophys. J.* **152**, 465–476, 1968.
- [3] A. T. Young, E. F. Milone, and C. R. Stagg, "On Improving IR Photometric Passbands," in *Stellar Photometry — Current Techniques and Future Developments*, C. J. Butler and I. Elliott, eds., (IAU Colloquium 136) Cambridge University Press, Cambridge, pp. 235–241, 1993.
- [4] A. T. Young, E. F. Milone, and C. R. Stagg, "On Improving IR Photometric Passbands," *Astronom. Astrophys. Suppl.* **105**, 259–279, 1994.
- [5] D. A. Simons and A. Tokunaga, "The Mauna Kea Observatories Near-Infrared Filter Set. I. Defining Optimal 1–5 Micron Bandpasses," *Pub. Astronom. Soc. Pacific* **114**, 169–179, 2002.
- [6] A. T. Tokunaga, D. A. Simons, and W. D. Vacca, "The Mauna Kea Observatories Near-Infrared Filter Set. II. Specifications for a New *JHKL'M'* Filter Set for Infrared Astronomy," *Pub. Astronom. Soc. Pacific* **114**, 180–186, 2002.
- [7] E. F. Milone and A. T. Young, "An improved infrared passband system for ground-based photometry: realization," *Pub. Astronom. Soc. Pacific* **117**, 485–502, 2005.
- [8] E. F. Milone and A. T. Young, "Standardization and the Enhancement of Infrared Precision," in *The Future of Photometric, Spectrophotometric, and Polarimetric Standardization*, C. Sterken, ed., (ASP Conf. Series, vol. 364) Astronomical Society of the Pacific, San Francisco, pp. 387–407, 2007.
- [9] E. F. Milone and A. T. Young, "Infrared passbands for precise photometry of variable stars by amateur and professional astronomers," *J. American Assoc. Variable Star Observers* **36**, no. 1, 110–126, 2008.
- [10] R. L. Kurucz, "New atmospheres for modelling binaries and disks," in *Light Curve Modeling of Eclipsing Binary Stars*, E. F. Milone, ed. Springer-Verlag, New York, pp. 93–101, 1993.
- [11] E. F. Milone, C. R. Stagg, and A. T. Young, "Towards robotic IR observatories: improved IR passbands," in *Robotic Observatories*, M. F. Bode, ed. Wiley/Praxis, Chichester, pp. 117–124, 1995.
- [12] J. D. Forbes, "On the transparency of the atmosphere and the law of extinction of the solar rays in passing through it," *Phil. Trans.* **132**, 225–273, 1842.
- [13] A. T. Young, "Extinction and Transformation," in *Infrared Extinction and Standardization*, E. F. Milone, ed., (Lecture Notes in Physics, vol. 341) Springer-Verlag, Berlin, pp. 6–14, 1989.
- [14] M. J. Selby, I. Hepburn, D. E. Blackwell, A. J. Booth, D. J. Haddock, S. Arribas, S. K. Leggett, and C. M. Mountain, "Narrow band 1 μm –4 μm infrared photometry of 176 stars," *Astronomy and Astrophysics Supplement Series* **74**, 127–132, 1988.
- [15] C. Sterken and J. Manfroid, *Astronomical Photometry: A Guide (Astrophysics and Space Science Library, Vol. 175)*, Kluwer, Dordrecht, p. 169, 1992.
- [16] M. F. Skrutskie, R. M. Cutri, R. Stiening, M. D. Weinberg, S. Schneider, J. M. Carpenter, C. Beichman, R. Capps, T. Chester, J. Elias, J. Huchra, J. Liebert, C. Lonsdale, D. G. Monet, S. Price, P. Seitzer, T. Jarrett, J. D. Kirkpatrick, J. E. Gizis, E. Howard, T. Evans, J. Fowler, L. Fullmer, R. Hurt, R. Light, E. L. Kopan, K. A. Marsh, H. L. McCallon, R. Tam, S. Van Dyk, and S. Wheelock, "The two micron all sky survey (2MASS)," *AJ* **131**, 1163–1183, 2006.
- [17] E. F. Milone and A. T. Young, "The Rise and Improvement of Infrared Photometry," in *Astronomical Photometry: Past, Present, & Future*, E. F. Milone and C. Sterken, eds. Springer, New York, pp. 125–141, 2011.
- [18] E. F. Milone, *Infrared Extinction and Standardization (Lecture Notes in Physics, Vol. 341)*, Springer-Verlag, Berlin, 1989.
- [19] E. F. Milone and J. Kallrath, "The Tools of the Trade and the Products they Produce: Modeling of Eclipsing Binary Observables," in *Short-Period Binary Stars: Observations, Analyses, and Results*, Springer, Berlin, pp. 191–214, 2008.